Processing of digital holograms for size measurements of microparticlese

Naughton, Thomas J.; Darakis, Emmanouil; Khanam, Taslima; Rajendran, Arvind; Kariwala, Vinay; Asundi, Anand Krishna

2008

Darakis, E., Khanam, T., Rajendran, A., Kariwala, V., Asundi, A. K., & Naughton, T. J. (2008). Processing of digital holograms for size measurements of microparticlese. Proceedings of SPIE-Ninth International Symposium on Laser Metrology, 7155.

https://hdl.handle.net/10356/96102

https://doi.org/10.1117/12.814578

Processing of digital holograms for size measurements of microparticles

Emmanouil Darakis,[c,a] Taslima Khanam,[a] Arvind Rajendran,[a] Vinay Kariwala,[a]
Anand K. Asundi,[b] and Thomas J. Naughton.[c,d]
[a]School of Chemical and Biomedical Engineering, Nanyang Technological University, Singapore, 637459;
[b]School of Mechanical and Aerospace Engineering, Nanyang Technological University, Singapore, 639798;
[c]Department of Computer Science, National University of Ireland, Maynooth, County Kildare, Ireland;
[d]University of Oulu, RFMedia Laboratory, Oulu Southern Institute, Vierimaantie 5, 84100 Ylivieska, Finland.

ABSTRACT

Digital holography has been reported as an effective tool for particle analysis. Other image-based techniques have small depth of focus allowing only 2D analysis at microscopic level. On the other hand, digital holography offers the ability to study volume samples from a single recording as reconstructions at different depths can be obtained. This paper focuses on the processing of the digital hologram that follows its recording in order to obtain particle size. We present a step-wise processing procedure with discussion on aspects such as reconstruction, background correction, segmentation, focusing, magnification and particles' feature extraction. Solutions to common obstacles faced during particle analysis which include ways to obtain fixed size reconstructions, automatically determine the threshold value, calculate magnification, and locate particles' depth position using effective focusing metrics are highlighted. Real holograms of microparticles are used to illustrate and explain the different stages of the procedure. Experimental results show that the proposed algorithm can effectively extract particle size information from recorded digital holograms.

Keywords: Digital holography, microparticle analysis, particle size distribution measurement.

1. INTRODUCTION

Several applications require the precise measurement of the position, speed or the size distribution of particles or other micro objects suspended in gas or liquid mediums. Imaging based particle analysis techniques suffer from the reduced depth of field imposed by the required magnification. As a result they can only be used to study particles on very thin volumes and have increased number of false positive identifications corresponding to out of focus particles.[1,2] Holographic particle analysis is an established technique for particle measurements.[3] The use of high definition photographic films for the recording of particle holograms allows the study of samples with relatively large volumes and with high resolution but suffers from increased processing time required for film development and subsequent digitization of the reconstructions. With digital recording of holograms, the chemical processing step for the film development is eliminated, which substantially increases the practicability of the method.[4-6] The resolution achievable by digital holographic systems might not be as high as the one obtained with holograms recorded on high resolution films, but the ease of processing has made digital holography more attractive.

The recording of digital holograms for particle analysis is discussed in the literature.[4,6,7] Similar techniques have been used for several applications including the study of plankton in sea water[8] and holographic particle image velocimetry.[9] This paper reviews several aspects of digital holographic analysis for particle size measurements and

Further author information: E. Darakis: emmdarakis@ieee.org, T. Khanam: tasl0001@ntu.edu.sg, A. Rajendran: arvind@ntu.edu.sg, V. Kariwala: vinay@ntu.edu.sg, A. K. Asundi: anand.asundi@pmail.ntu.edu.sg, T. J. Naughton: tomn@cs.nuim.ie

Ninth International Symposium on Laser Metrology, edited by Chenggen Quan, Anand Asundi
Proc. of SPIE Vol. 7155, 715524, (2008) · 0277-786X/08/$18 · doi: 10.1117/12.814578

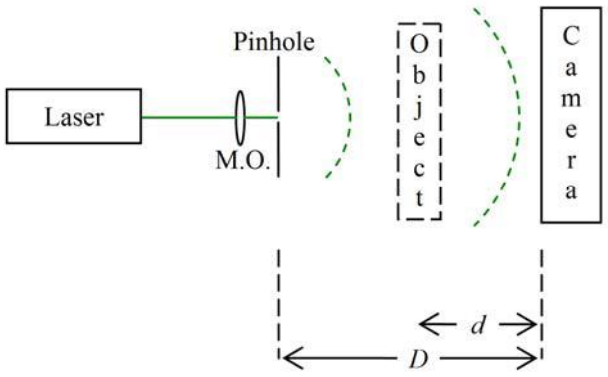

Fig. 1. Digital holographic microscopy setup. M. O. stands for microscopic objective lens.

focuses on the processing required following the recording of the digital hologram in order to identify and measure the recorded particles. The aim is to design an effective and accurate automated algorithm capable of extracting particles from digital holograms with the fewest possible tuning parameters and without any other assumptions about the size or the shape of the particles under consideration. Following this, the algorithm should be able to accurately measure properties of the extracted particles such as their size and shape. In this paper, we focus only on particle size distribution (PSD) and results about particle shape such as axis length distribution (ALD) obtained using the same algorithm are discussed elsewhere.[10]

Direct fringe analysis based methods for estimating the size or the focusing point of particles recorded in digital holograms without reconstruction have been reported,[11-13] but these methods are only applicable in the case of spherical particles and hence are not considered in this paper. Our method uses edge detection[14] to segment the particles from reconstructions at several depths. The best focusing depth for each particle is identified based on a focusing metric. Following focusing, the size and the shape of the particles are estimated.

In order to verify the performance of the algorithm, several experiments with real particle holograms have been performed and the obtained experimental results are discussed. In particular, we present experiments verifying the focusing algorithm. In addition, we have measured the PSD of a population of particles with varying size using the proposed algorithm and we compare the results with corresponding results obtained from scanning electron microscope (SEM) images of particles from the same population. Finally, a number of particles with very narrow size distribution suspended in water is examined and the obtained PSD are compared to the expected ones. The experimental results verify that the algorithm can be used to accurately measure particles of sizes down to $10\,\mu m$ with an error of $\sim 5\,\mu m$.

The paper is organized as follows: In Section 2, the in-line digital holographic microscopy recording setup is described together with the fundamentals of digital holography. In Section 3, the algorithm that is used for the processing of the recorded digital holograms is described in details followed by Section 4, where the results obtained from the experiments used to verify the accuracy and the effectiveness of the algorithm are presented and Section 5 concludes the paper.

2. IN-LINE DIGITAL HOLOGRAPHIC MICROSCOPY

2.1 In-line digital holographic recording setup

The setup that has been used for the recording of the digital holograms is shown in Fig. 1. A laser beam is focused by a microscopic objective lens on a pinhole which is located at a distance D from the recording camera. The resulting spherical diverging reference beam illuminates the sample which is located at a distance d from the recording camera. One part of the illuminating beam passes through the sample without being diffracted and acts as the reference beam U_R. The spherical diverging reference beam can be expressed as[4]

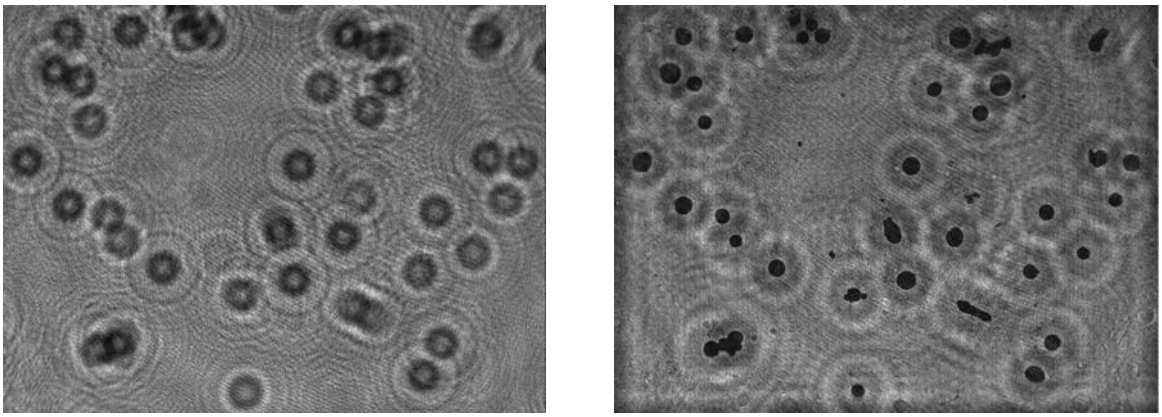

(a) (b)

Fig. 2. Digital holographic microscopy data of ceramic beads on a slice. (a) recorded digital hologram; and (b) a reconstruction.

$$U_R(x,y) = \frac{\exp\left(-i\frac{2\pi}{\lambda}\sqrt{x^2+y^2+D^2}\right)}{\sqrt{x^2+y^2+D^2}}, \tag{1}$$

where x and y are the spatial coordinates on the camera plane and λ is the wavelength of the laser beam. Another part of the illuminating beam is diffracted by the particles within the sample generating the object beam U_d which propagates towards the recording camera. The object beam at the camera plane can be expressed by the Fresnel-Kirchhoff integral as[4]

$$U(x,y) = \int_{-\infty}^{+\infty}\int_{-\infty}^{+\infty} U_d(x',y')\frac{\exp\left[-i\frac{2\pi}{\lambda}\sqrt{(x'-x)^2+(y'-y)^2+d^2}\right]}{\sqrt{(x'-x)^2+(y'-y)^2+d^2}}dx'dy', \tag{2}$$

where x' and y' are the spatial coordinates on the object plane. In Eq. (2) constant phase terms have been omitted for simplicity. The interference pattern between the reference and the object waves is captured by a digital camera and can be expressed as

$$I(x,y) = \left[U_R(x,y) + U(x,y)\right]^2. \tag{3}$$

Fig. 2(a) shows a recorded digital hologram. In order to reconstruct the hologram at a distance d', I needs to be multiplied by the reference wave and then propagated using the Fresnel-Kirchhoff integral as[4]

$$U_{d'}(x',y') = \int_{-\infty}^{+\infty}\int_{-\infty}^{+\infty} I(x,y)U_R(x,y)\frac{\exp\left[-i\frac{2\pi}{\lambda}\sqrt{(x-x')^2+(y-y')^2+d'^2}\right]}{\sqrt{(x-x')^2+(y-y')^2+d'^2}}dxdy. \tag{4}$$

For $d' = d$, when quantization and other digitizing errors are negligible, the reconstructed wave $U_{d'}$ equals the object wave U_d. Fig. 2(b) shows a reconstruction obtained from the hologram shown in Fig. 2(a).

2.2 Digital holographic microscopy reconstruction

In digital holographic microscopy, Eq.(4) has to be numerically calculated with the convolution reconstruction method in which case, the pixel size of the reconstructed image $(\Delta x', \Delta y')$ equals the pixel size of the recording

camera $(\Delta x, \Delta y)$, i.e. $\Delta x' = \Delta x$ and $\Delta y' = \Delta y$.[4] Lateral magnification defined as $M(d) = r'(d)/r$, where $r'(d)$ is the measured object size at distance d and r is the real object size, can be introduced by changing the distance between the source of the spherical reference wave and the CCD, or the wavelength that is used for the reconstruction as[4]

$$M(d) = \left(1 + \frac{d}{D'}\frac{\lambda}{\lambda'} - \frac{d}{D}\right)^{-1}, \tag{5}$$

where D' is the pinhole to CCD distance and λ' is the wavelength that are used for the reconstruction respectively. By changing D' and λ', the distance d' where the object will appear focused also changes as[4]

$$d' = \left(\frac{1}{D'} + \frac{\lambda'}{\lambda}\frac{1}{d} - \frac{1}{D}\frac{\lambda'}{\lambda}\right)^{-1}. \tag{6}$$

For our experiments we only change D' as $D' = 100D$ and retain $\lambda' = \lambda$.

The digital holography setup which has been described above has three desirable characteristics. Firstly, it can magnify the reconstructed object wave allowing the study of smaller particles compared to systems which use collimated illumination. Secondly, it minimizes the effects of the twin image since the twin image is well out of focus for the depths where the particles appear focused.[7] Finally, the described reconstruction method simplifies the spatial localization of the particles as it overcomes the pixel resizing problem which causes shifting of the $x-y$ location of the particles for different depth reconstructions.

3. DIGITAL HOLOGRAM PROCESSING FOR PARTICLE MEASUREMENTS

Algorithms to extract particle size and location information from digital holograms without reconstruction assume spherical particle size and cannot be used for our study.[11-13] Hence, in order to study a volume of the sample, each hologram needs to be reconstructed at several reconstruction depths. Our method is summarized as follows:

1. The recorded hologram is reconstructed at several depths covering the volume to be studied with sufficiently small depth steps.
2. For each reconstruction, edge detection is used to identify particles. The location, area, and focusing metric for each identified particle are recorded.
3. Each particle may be identified on several depths. Occurrences of the same particle at different depths are identified by examining their $x-y$ location on the reconstruction plane.
4. Based on the focusing metric, the best focusing depth is identified for each particle.
5. Following focusing, the size and the shape of the particles can be estimated.

The distance between successive reconstructions depends on the minimum size of the particles to be studied. In general, this distance should be similar to the minimum particle size that needs to be identified, if not smaller. The details of the algorithm are described in the following sections.

3.1 Preprocessing and background correction

As shown in Fig. 2(b) the background of the reconstructed hologram is not uniform. The bright background is due to the zero order of the reconstruction which is also contaminated by noise caused by speckle due to the coherent illumination, the twin image and non uniform illumination. One approach to reduce the zero order term from the reconstruction is to high-pass the hologram with a low-cutoff frequency filter before reconstruction.[4] Another approach is to record the reference wave (without the object) and subtract it from the hologram prior to reconstruction.[7] This approach however, is impractical for real time monitoring systems as the sample needs to be removed from the system regularly in order to record updated images of the reference wave. In all cases, we have noticed that the suppression of the zero order term affects the particles, by blurring or changing their perimeter, leading to erroneous size measurements. As a result, these approaches offer practical disadvantages. In the following section, we propose an edge detection-based technique for particle segmentation which is immune to zero order and other irregularities of the background, thus eliminating preprocessing of the hologram.

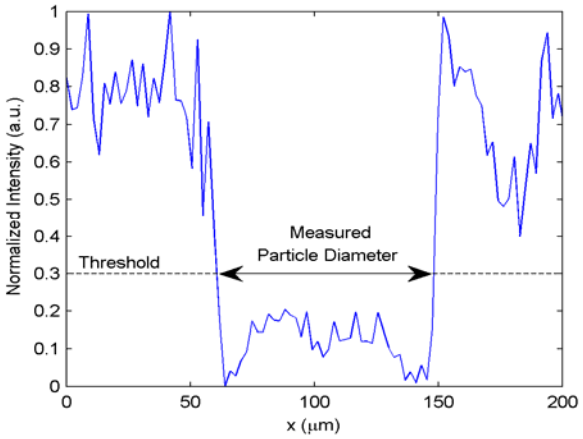

Fig. 3. A cross-section of normalized intensity around a particle and a threshold value used for segmentation. The selection of the threshold value affects the measured particle's diameter.

3.2 Particle segmentation

3.2.1 Threshold-based segmentation

Segmentation can be performed by thresholding the intensity of the reconstruction.[15] Pixels with intensity value lower than the threshold are considered to belong to a particle while any pixels with higher intensity values than the threshold are considered to belong to the background. This approach has several drawbacks related to the selection of the threshold value.

A manual threshold selection can be done, but this would limit the usefulness of the method as input from the user would be required for every processed hologram. A threshold value can be calculated but knowledge of the median background intensity, the standard deviation of the background noise, and the expected size of the particles need to be assumed.[15] Histogram-based approaches can also be utilized for automatic threshold selection.[16] The histogram of the reconstruction intensity is expected to have 2 distinct peaks, one corresponding to dark areas (particles) and another corresponding to the bright areas (background). The threshold can then be selected as the value where the histogram valley between these peaks is located. However, reconstructed digital holograms suffer from increased noise causing several minima and maxima in the intensity histogram. As a result such histogram-based techniques usually fail to locate an adequate threshold value. Noise removal[17] can reduce these effects but still multiple minima and maxima cannot be eliminated from the histogram.

Even if a threshold value could be determined, manually or automatically, other factors such as variations of the zero order term in the reconstruction and irregular illumination prevent its use for accurate segmentation. Also as it can be seen in Fig. 3, a different threshold value changes the measured diameter of the particle, limiting the measurement accuracy. As a result, threshold-based segmentation methods offer limited accuracy in the case of digital holography and are not considered here.

3.2.2 Edge detection-based segmentation

In order to increase accuracy, we use the Canny edge detection technique which locates edges by examining gradients after a Gaussian filtered has been applied to the reconstruction.[14] Gaussian filtering reduces the effect of noise on erroneous identification of edges. Following Gaussian filtering, the edge detection algorithm examines the derivatives for local maxima. Thresholding with hysteresis is used to classify the identified maxima. Two thresholds t_L and t_H are used for this. Maxima with a value lower than t_L are identified as not being edges immediately. Maxima with a value higher than t_H are identified as edges immediately too. Maxima with value between t_L and t_H are identified as edges only if they are connected to identified edges. The algorithm results in a set of ones ('1') where edges have been detected and zeros everywhere else.

The method requires the selection of 3 parameters. The standard deviation σ and the two thresholds t_L and t_H. σ is selected so that the filtering operation does not alter the size of the particles that need to be examined. A large standard

deviation results in a Gaussian filter with large length which may affect the size of small particles causing erroneous size measurements. The thresholds t_L and t_H on the other hand affect only the number of particles to be identified and not their size. High values lead to identification of fewer particles (only those with very sharp edges), while lower values increase the number of identified particles but also might lead to false positives (areas which happen to be surrounded by strong edges). Such areas correspond to fringes caused by the virtual image or out of focus particles and are much brighter than focused particles. As a result, they can be easily identified and neglected based on their average intensity.

The selection of these parameters is not critical for the performance of the algorithm and they do not have to be tuned for each hologram. This is verified by the results presented in Section 4 where the same set of parameters has been found to give acceptable results for all the experiments which cover a large number of holograms recorded under different conditions and depicting different particle sizes.

Following edge detection, the dark areas that are completely enclosed by edges are filled in to form blobs that are considered as possible particles. Open ended lines are removed by erosion followed by dilation in order to eliminate noisy formations that frequently appear in the background. This does not change the size of the identified blobs. Blobs that are touching the edges of the reconstruction correspond to partially shown particles and are therefore removed in order to avoid size measurements corresponding to partial particles. Also blobs with very small diameter are removed as are likely to correspond to noise.

Apart from good localization, the use of edge detection-based particle segmentation on digital holograms also has the advantage that particles are surrounded by strong edges only close to their best focusing point. As a result, highly unfocused particles are not considered easing depth localization. The procedure described above results in a set of blobs which correspond to particles shown in the reconstruction. These blobs have the same size and shape as the corresponding particles and can be use for particle measurement as discussed in Section 3.4.

3.3 Particle focusing

As it can be seen from Eq.(5), magnification depends on the object distance from the camera. On the other hand, it is practically impossible to know the exact location of the particles within the sample, hence this distance need to be accurately determined from the recorded hologram for each particle separately. Direct interferogram analysis methods[11-13] assume circular particles and hence cannot be used. As a result, reconstructions corresponding to several distances have to be obtained and then the best focusing distance for each particle has to be identified separately using a focusing metric. Mean intensity and the variance of the intensity have been reported as an appropriate focusing methods.[7,18]

The focusing algorithm is as follows:

1. Following segmentation of each reconstruction, the focusing metric is calculated and stored for each identified blob separately.
2. Once this has been done for all the blobs and reconstruction distances, blobs which have overlapping spatial positions at different depths are labeled as one particle.
3. The depth profile of the focusing metric is formed for each particle.
4. The best focusing depth for each particle is selected as the depth where the focusing metric is minimized.

Normalized depth profiles of the mean intensity and the variance of the intensity for one particle are shown in Fig. 4. In this case the best focusing depth is 36 mm. There are cases where the minimum of the particle's depth profile appears at the last or the first examined depth. In these cases, the particle is probably located outside the examined depth range and hence such particles are ignored to avoid erroneous measurements.

3.4 Particle size measurement

Following segmentation and particle focusing, the area which each particle occupies at its best focusing depth is determined accurately. In general, the particles are not spherical and as a result the identified regions are not circular. As a result, it is not always easy to measure their sizes. However, several properties of these areas can be extracted for further size and shape analysis. For example, the equivalent diameter (the diameter of a circle with the same area as the identified region) can be used to extract the PSD of the particles. The measured PSD will be correct assuming that the particles are close to circular. Also an ellipse with the same normalized second central moment as the identified region can be used to calculate the lengths of the major and the minor axes. Assuming that the identified ellipses characterize

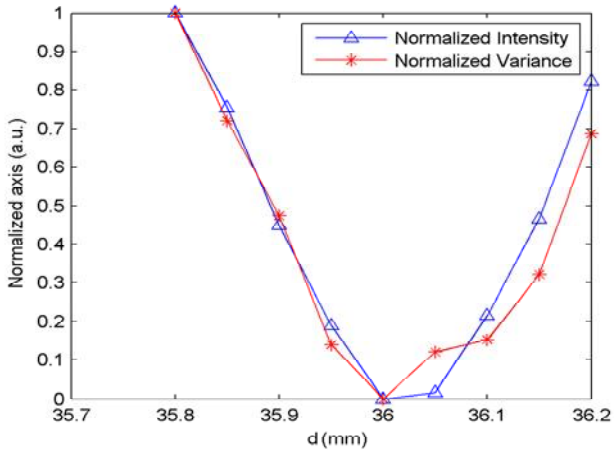

Fig. 4. Depth profile of the normalized focusing metrics (mean intensity and variance of the intensity) for one particle. The best focusing depth for this particle is 36 mm.

the particles, these lengths can be used to calculate ALD, or to differentiate between circular, ellipsoidal, and needle-like particles.

In order to convert the measured size to real length, the value needs to be converted using the magnification factor M as

$$r = \frac{r_{pixels}\Delta x}{M(d_o)}, \tag{7}$$

where r_{pixels} is the measured size of the particle in pixels and d_o is the best focusing depth of each particle.

4. EXPERIMENTS AND RESULTS

In this section, several experiments are presented to verify the performance of algorithms described in Section 3. This paper focuses on particle measurement results. Results of shape measurement obtained using this algorithm are shown in another paper.[10] Section 4.1 describes an experiment that is used to verify the accuracy of the focusing step. Sections 4.2 to 4.4 present other experiments which verify the performance and the accuracy of the whole particle measurement procedure.

Three particle populations were examined:

- A population of ceramic beads with a large diameter range (~ 50 μm to ~ 150 μm). The average diameter of the population was ~ 80 μm.
- A population of polymer microspheres with a certified diameter of 40 μm.
- A population of polymer microspheres with a diameter of 10 μm.

The ceramic beads could not be suspended in water as their density was too high, hence they have been used only for experiments requiring a dry sample, such as the experiments described in Sections 4.1 and 4.2. A glass slide was used to hold the sample for digital holography experiments and the sample holder of the SEM instrument for the SEM experiments. The polymer microsphere particles were suspended in water, hence they were used in the cases where a volume sample was needed (Sections 4.3 and 4.4). For these experiments the sample was contained in a cuvette. The length of the cuvette along the optical axis was 1 cm.

For the digital holographic microscopy experiments the recording setup shown in Fig. 1 was used with a green laser $(\lambda = 532\,\text{nm})$, a $60\times$ microscopic objective and 1 μm pinhole. The distance between the point source and the CCD

camera for the recording was approximately $D = 62$ mm and for the reconstruction, a point source to CCD camera distance of $D' = 100D = 6.2$ m was used. The camera used for the experiments had 1280×960 square pixels of size $\Delta x = \Delta y = 4.65$ μm. Prior to the described experiments the setup was tested with a USAF target. The obtained resolution for $D = 62$ mm was ~7 μm. The theoretical magnification of the setup according to Eq.(5) was also experimentally verified.

The threshold values that were used for the edge detection algorithm for all the experiments were chosen as $t_L = 0.3$ and $t_H = 0.6$. The standard deviation of the Gaussian filter used for the edge detection in the experiments described in Sections 4.1, 4.2, and 4.3 was selected as $\sigma = 1.5$ which results in a filter size of 6×6 pixels. This filter length has been found to give good noise reduction without affecting the size of the smallest particles studied in these experiments which had a diameter of 40 μm or ~17 pixels particles. In the experiments described in Section 4.4, particles with a diameter of 10 μm or ~3 pixels were studied. Due to the small size of these particles, no Gaussian filtering was used prior to edge detection. Nevertheless it is shown in Section 4.4 that the algorithm was still able to detect the particles and measure their size with acceptable levels of accuracy.

4.1 Verification of the focusing algorithm

In order to verify the accuracy of the focusing method a series of experiments were carried out. For these experiments, the object consisted of seven ceramic beads with sizes ~80 μm positioned on a glass slide. The slide was positioned in the setup normal to the optical axis so that the particles were located at the same depth and a hologram was captured. The slide was then consecutively displaced by 1 mm along the optical axis every time, and a hologram was recorded for each displacement. The experiment was then repeated for a slide displacement of 0.1 mm. In both cases, the displacement was achieved with a device that had an accuracy of ±0.1 mm.

Following this, the focusing algorithm was used to find the best focusing point for the particles of each hologram. In the case of 1 mm displacement, the algorithm was used to find the best focusing point within a depth range of 27.5 to 32.5 mm and in the case of 0.1 mm within a range of 20 to 34 mm. In both cases, the depth step was selected as 50 μm. Following the focusing of the particles the depth of the slide for each position was estimated by averaging the depth of the particles. **Error! Reference source not found.** shows the measured slide positions. The best focusing depth of the particles and the estimated slide positions are shown in Fig. 5(a) for the displacement of 1 mm and in Fig. 5(b) for the displacement of 0.1 mm.

According to Table 1, the maximum observed error between the measured and the expected slide displacement is 120 μm. Also, assuming that all the particles are located at the same depth as the slide, the maximum observed error between a particle's depth and the corresponding slice depth is 110 μm as it can be seen in Fig. 5. According to Eq.(5), a 110 μm focusing error causes an error in magnification of ~0.35% under these conditions.

4.2 Comparison with Scanning Electron Microscopy

In order to verify the performance of the particle measurement algorithm, we studied ceramic beads from a population with a wide range of sizes around 80 μm. Several holograms of particles from the population positioned on glass slides were recorded using the setup shown in Fig. 1. The recorded holograms were processed following the procedure described in Section 3. A depth of 3 mm with a step size of 50 μm was used for each hologram. The algorithm identified 437 different particles.

In addition, an SEM was used to record several images of different particles taken from the same population. One such image is shown in Fig. 6(a). The SEM images were segmented using Canny edge detection, using the same parameters as before, to extract the particles (bright areas) and the size of each particle was measured considering the magnification of the SEM. 615 different particles were measured from the SEM captured images.

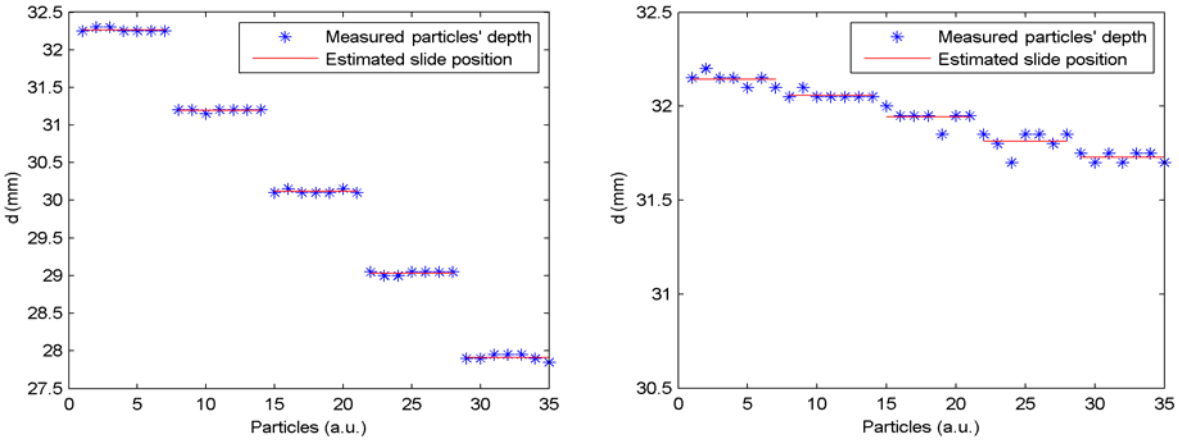

(a) (b)

Fig. 5. Verification of the focusing algorithm (a) for 1 mm displacement and (b) for 0.1 mm. Asterisks show the measured position of the particles (d_o) and the lines show the estimated slide depth (average depth of the particles).

Table 1. Numerical results of the focusing algorithm for displacement of (a) 1 mm and (b) 0.1 mm.

d (mm)	Measured Displacement (mm)	Expected Displacement (mm)	Error (mm)
32.26	-	-	-
31.19	1.07	1	0.07
30.11	1.08	1	0.08
29.03	1.08	1	0.08
27.91	1.12	1	0.12

(a)

d (mm)	Measured Displacement (mm)	Expected Displacement (mm)	Error (mm)
32.14	-	-	-
32.06	0.08	0.1	-0.02
31.94	0.12	0.1	0.02
31.81	0.13	0.1	0.03
31.73	0.08	0.1	-0.02

(b)

Fig. 6(b) shows the resulting PSD measurements from the holography and the SEM experiments. The mean particle size identified from the holographic microscopy and the SEM were 81.1 μm and 79.2 μm respectively and their standard deviation were 14.2 μm and 13.9 μm respectively. In the case of SEM focusing was performed manually during the recording, and the magnification was provided automatically from the instrument. On the other hand, in the case of digital holography, focusing and the calculation of the magnification factor was performed by the algorithm. The results of this experiment verified the accuracy of the digital hologram based measurement algorithm.

4.3 Microparticles suspended in water (average diameter of 40 μm)

The experiments described in Sections 4.1 and 4.2 verify that the algorithm can effectively locate particles and accurately measure their sizes. For this experiment, particles with certified diameter of 40 μm suspended in water were examined. One hologram was recorded from the sample. The hologram was reconstructed at 200 different depths with a distance of 25 μm from each other so that an overall depth of 0.5 cm was covered. 42 different particles were identified.

Fig. 7(a) shows one reconstruction of the hologram and Fig. 7(b) the calculated PSD. There is an error of ~5 μm between the actual particle size and the location of the PSD peak. This error is below the resolution of the system and it can also be partially attributed to inaccurate measurement of the distance D between the point source and the recording

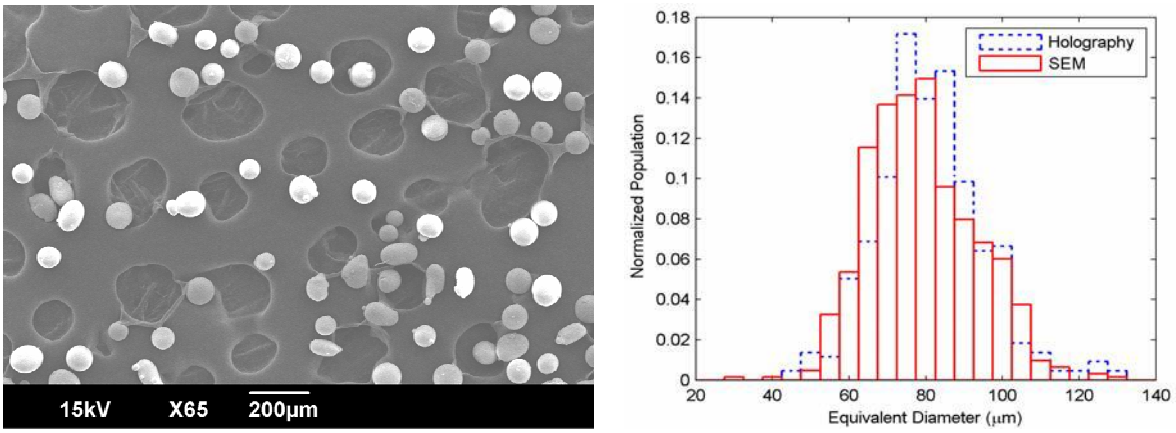

(a) (b)

Fig. 6. (a) An image of ceramic beads obtained from the SEM. Bright areas correspond to particles whereas the dark circular areas on the background are irregularities of the sample holder. (b) Comparison of PSD obtained from digital holography and SEM.

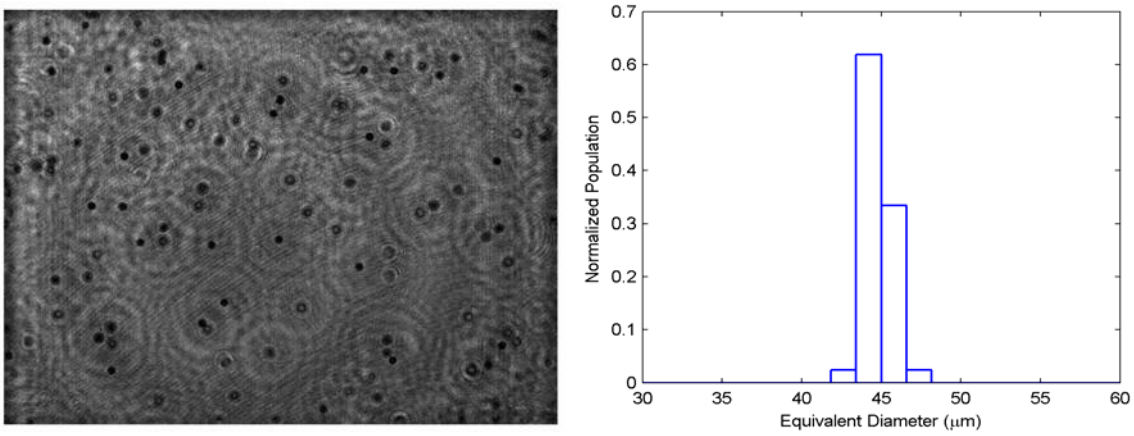

(a) (b)

Fig. 7. Digital hologram of 40 µm particles suspended in water: (a) example of reconstruction; and (b) measured PSD from 42 particles.

camera, which for practical reasons, cannot be measured accurately.

4.4 Microparticles suspended in water (average diameter of 10 µm)

In this experiment, 10 µm particles suspended in water were examined. 40 reconstructions with a distance of 25 µm between each other were obtained from one hologram to cover a depth of 1 mm. 47 different particles were identified from the algorithm. Fig. 8(a) shows one reconstruction of the hologram and Fig. 8(b) the calculated PSD. The particle size is very close to the resolution limit of the system (~7 µm) leading to the relatively large spread around the expected size which can be seen in Fig. 8(b).

The experiments presented in Sections 4.3 and 4.4 verify the performance of the algorithm, when applied to holograms recorded from particles suspended in water. As it can be seen in Fig. 7(a) and Fig. 8(a), the presence of the

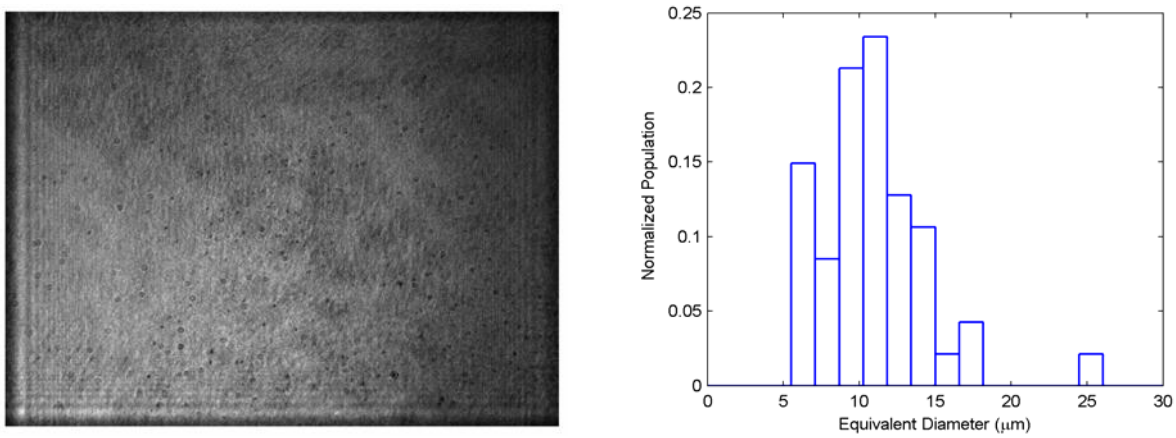

(a) (b)

Fig. 8. Digital hologram of 10 μm particles suspended in water: (a) example of reconstruction; and (b) measured PSD from 47 particles.

cuvette and the water does not change the reconstructed holograms significantly and hence the performance of the algorithm is not affected.

5. CONCLUSIONS

In this paper, a particle size measurement methodology based on digital holographic microscopy was presented. The steps of the measuring procedure were described in details. Apart from the known parameters related to the recording (such as the wavelength and the reconstruction distance), and the minimum size of particles to be identified, the method requires the selection of a small set of unknown parameters, namely the standard deviation of the Gaussian filter, and the threshold values needed for the edge detection. No assumptions on aspects such as the shape of the particles were used for the identification.

A series of digital holographic microscopy experiments using holograms of real particles were used in order to verify the algorithm. The results revealed that the method can measure particles as small as 10 μm with an error of ~5 μm which is close to the resolution of the system used. It has also been demonstrated that the method is able to identify dry particles and particles suspended in water. Finally, the experiments showed that the selection of the parameters (standard deviation of Gaussian filter, and edge detection thresholds) is not crucial for the performance of the algorithm, as the same values can be used under several different circumstances giving satisfactory results.

ACKNOWLEDGMENTS

This work was partially funded by the Irish Research Council for Science, Engineering and Technology under the National Development Plan through grant no. PD/2007/11 and partially by the Office of Research, Nanyang Technological University through grant no. RG25/07. The authors would also like to thank Vijay Raj Singh and Qu Weijuan for assisting with the recording setup.

REFERENCES

[1] Kempkes, M., Eggers, J. and Mazzotti, M., "Measurement of particle size and shape by FBRM and in situ microscopy," Chem. Eng. Sci., In Press, 2008.

[2] Wang, X. Z., Roberts, K. J. and Ma, C., "Crystal growth measurement using 2D and 3D imaging and the perspectives for shape control," Chem. Eng. Sci., vol. **63**, pp. 1173-1184, 2008.

[3] Vikram, C. S., [Particle field holography], Cambridge University Press, Cambridge, 1992.

[4] Schnars, U. and Juptner, W., [Digital Holography: Digital Hologram Recording, Numerical Reconstruction, and Related Techniques], Springer, Berlin, 2005.
[5] Frauel, Y., Naughton, T. J., Matoba, O., Tajahuerce, E. and Javidi, B., "Three-dimensional imaging and processing using computational holographic imaging," Proc. IEEE, vol. **94**, pp. 636-653, 2006.
[6] Asundi, A. and Singh, V. R., "Circle of Holography—Digital In-Line Holography for Imaging," J. Holography Speckle, vol. **3**, pp. 106-111, 2006.
[7] Xu, W., Jericho, M. H., Meinertzhagen, I. A. and Kreuzer, H. J., "Digital in-line holography of microspheres," Appl. Opt., vol. **41**, pp. 5367-5375, 2002.
[8] Sun, H., Hendry, D. C., Player, M. A. and Watson, J., "In Situ Underwater Electronic Holographic Camera for Studies of Plankton," IEEE J. Oceanic Eng., vol. **32**, pp. 373-382, 2007.
[9] Hinsch, K. D., "Holographic particle image velocimetry," Meas. Sci. Technol., vol. **13**, p. R61, 2002.
[10] Khanam, T., Darakis, E., Rajendran, A., Kariwala, V., Naughton, T. J. and Asundi, A. K., "On-line digital holographic measurement of size and shape of microparticles for crystallization processes," in Proceedings of the 9th International Symposium on Laser Metrology, A. K. Asundi, Ed. SPIE, 2008.
[11] Buraga-Lefebvre, C., Coetmellec, S., Lebrun, D. and Ozkul, C., "Application of wavelet transform to hologram analysis: three-dimensional location of particles," Opt. Laser Eng., vol. **33**, pp. 409-421, 2000.
[12] Denis, L., Fournier, C., Fournel, T., Ducottet, C. and Jeulin, D., "Direct extraction of the mean particle size from a digital hologram," Appl. Opt., vol. **45**, pp. 944-952, 2006.
[13] Soontaranon, S., Widjaja, J. and Asakura, T., "Extraction of object position from in-line holograms by using single wavelet coefficient," Optics Commun., vol. **281**, pp. 1461-1467, 2008.
[14] Canny, J., "A Computational Approach to Edge Detection," IEEE T. Pattern Anal., vol. **8**, pp. 679-698, 1986.
[15] Malkiel, E., Abras, J. N. and Katz, J., "Automated scanning and measurements of particle distributions within a holographic reconstructed volume," Meas. Sci. Technol., vol. **15**, p. 601, 2004.
[16] Shapiro, L. G. and Stockman, G. C., [Computer Vision], Prentice-Hall, New Jersey, 2001.
[17] Maycock, J., Hennelly, B. M., McDonald, J. B., Frauel, Y., Castro, A., Javidi, B. and Naughton, T. J., "Reduction of speckle in digital holography by discrete Fourier filtering," J. Opt. Soc. Am. A, vol. **24**, pp. 1617-1622, 2007.
[18] McElhinney, C. P., Hennelly, B. M. and Naughton, T. J., "Extended focused imaging for digital holograms of macroscopic three-dimensional objects," Appl. Opt., vol. **47**, 2008.